

A Polymeric Liquid Membrane Electrode Responsive to 3,3',5,5'-Tetramethylbenzidine Oxidation for Sensitive Peroxidase/Peroxidase Mimetic-Based Potentiometric Biosensing

Xuewei Wang,^{†,‡} Yangang Yang,[§] Long Li,^{†,‡} Mingshuang Sun,[§] Haogen Yin,[§] and Wei Qin^{*,†}

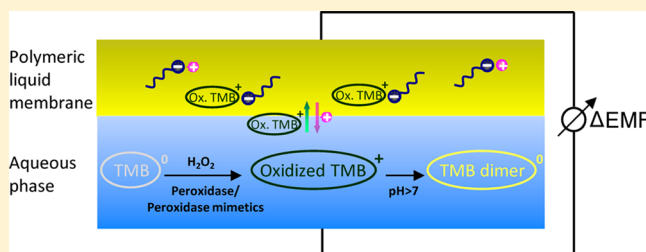
[†]Key Laboratory of Coastal Environmental Processes and Ecological Remediation, Yantai Institute of Coastal Zone Research (YIC), Chinese Academy of Sciences(CAS); Shandong Provincial Key Laboratory of Coastal Environmental Processes, YICCAS, Yantai, Shandong 264003, People's Republic of China

[‡]University of Chinese Academy of Sciences, Beijing 100049, People's Republic of China

[§]College of Chemistry and Chemical Engineering, Yantai University, Yantai, Shandong 264003, People's Republic of China

S Supporting Information

ABSTRACT: The oxidation of 3,3',5,5'-tetramethylbenzidine (TMB) has great utility in bioanalysis such as peroxidase/peroxidase mimetic-based biosensing. In this paper, the behaviors of TMB oxidation intermediates/products in liquid/liquid biphasic systems have been investigated for the first time. The free radical, charge transfer complex, and diimine species generated by TMB oxidation are all positively charged under acidic and near-neutral conditions. Electron paramagnetic resonance and visible absorbance spectroscopy data demonstrate that these cationic species can be effectively transferred from an aqueous phase into a water-immiscible liquid phase functionalized by an appropriate cation exchanger. Accordingly, sensitive potential responses of TMB oxidation have been obtained on a cation exchanger-doped polymeric liquid membrane electrode under mildly acidic and near-neutral conditions. By using the membrane electrode responsive to TMB oxidations, two sensitive potentiometric biosensing schemes including the peroxidase-labeled sandwich immunoassay and G-quadruplex DNAzyme-based DNA hybridization assay have been developed. The obtained detection limits for the target antigen and DNA are 0.02 ng/mL and 0.1 nM, respectively. Coupled with other advantages such as low cost, high reliability, and ease of miniaturization and integration, the proposed polymeric liquid membrane electrode holds great promise as a facile and efficient transducer for TMB oxidation and related biosensing applications.



The aromatic amine 3,3',5,5'-tetramethylbenzidine (TMB), which is noncarcinogenic and nonmutagenic, has been widely used as the peroxidase/peroxidase mimetic substrate for bioanalysis. TMB exhibits higher sensitivity and precision in peroxidase-based detection, compared to other substrates, such as *o*-phenylenediamine, benzidine, and 2,2'-azino-bis(3-ethylbenzthiazoline-6-sulfonic acid).¹ TMB oxidation has evolved to be one of the most commonly used reactions in biosensing schemes based on peroxidases and peroxidase mimetics (e.g., G-quadruplex DNAzymes and nanomaterials with peroxidase-like activities). A large number of sandwich and competitive bioaffinity assays using peroxidases or peroxidase mimetics as amplifying labels (e.g., peroxidase-linked immunoassays and nucleic acid hybridization assays) have been developed using TMB oxidation as the indicating reaction.² By monitoring target-modulated catalytic activities of peroxidase-mimicking DNAzymes and nanoparticles via TMB oxidation, sensing strategies for ions, nucleotides, nucleic acids, proteins, and cancer cells have also been proposed.³ In addition to peroxidases and peroxidase mimetics, TMB oxidation allows the detection of other biological and inorganic catalysts such as

hemoglobin, ferritin, iron and nitrite.⁴ Moreover, TMB has been used to probe various oxidants (e.g., H₂O₂, chlorine, and bromate)^{5,6} and reductants (e.g., glutathione, gold(I), manganese, and graphene radical).⁷ Especially, by sensing H₂O₂ generated by oxidase-catalyzed reactions, TMB oxidation can be used to indirectly detect analytically important chemicals such as glucose, melamine, xanthine, and organophosphates.⁵

The tremendous applications of TMB oxidation lead to considerable demands on facile and effective transduction techniques for this reaction. Visible absorption spectroscopy is the most commonly used technique, in which the optical absorbance of TMB oxidation products at 450 or 652 nm is used.^{5,6} Raman spectra of the diimine and charge-transfer complex products also allow the monitoring of TMB oxidation, and corresponding enzyme-linked immunosorbent assays and catalytic beacon-based DNA detection protocols have been developed with improved sensitivities, compared to the

Received: January 21, 2014

Accepted: April 7, 2014

Published: April 7, 2014



colorimetric methods.⁸ Although optical methods usually provide high throughput and high reliability, the cost-effective electrochemical techniques such as voltammetry and amperometry have been used to indicate TMB oxidation by utilizing the redox properties of the TMB oxidation products.⁹ Monitoring of this reaction by the quartz crystal microbalance has also been fulfilled based on the aqueous solubility change of TMB upon H_2O_2 -mediated oxidation.¹⁰ However, these techniques suffer from problems of inconvenient regeneration and activation steps on electrodes/quartz crystals, and of the regeneration-induced response deviations.

Polymeric liquid membrane electrodes are a type of sensor based on electrochemistry in liquid–polymeric liquid biphasic systems. They are traditionally used as potentiometric ion-selective electrodes working under thermodynamic equilibrium conditions, while nonclassical polymeric liquid membrane electrodes utilizing chemically or instrumentally controlled ion fluxes have also been developed in recent years.¹¹ With attractive features of portability, high reliability, low cost, and ease of miniaturization and integration, polymeric liquid membrane electrodes directly responsive to over 60 ions have been reported and they have found successful real-world applications in many important analytical aspects such as pH measurement, blood electrolyte analysis, and noninvasive ion microtest.¹¹ As an indirect application, ion-selective polymeric liquid membrane electrodes can be used to indicate biorecognition events such as immunoassays.¹² On the other hand, polymeric liquid membrane electrodes have been investigated as transducers of numerous analytically important chemical reactions by using potential signals of reactants, intermediates, and final products.¹³ The potentiometric indications of enzymatic and nonenzymatic redox, complexation, hydrolysis, and coupling reactions have been fulfilled by polymeric liquid membrane electrodes sensitive to H^+ , NH_4^+ , halogen ions, metal ions, organic ions, biological ions, and nonionic species.¹³ However, to the best of our knowledge, the sensing of TMB oxidation with polymeric liquid membrane electrodes has not been reported, although the TMB oxidation products are expected to be highly lipophilic and thereby well-suited to be detected by the lipophilic polymeric liquid membrane. Similarly, the sensing of TMB oxidation by electrochemistry at the interface between two immiscible electrolyte solutions has not been explored as well.

Here, we report the transfers of ionic intermediates/products involved in the TMB oxidation reactions across the liquid/liquid interface for the first time. Polymeric liquid membrane electrodes functionalized by cationic exchangers (i.e., lipophilic sulfonate or tetraphenylborate and its derivatives) as phase-transfer reagents have been found to show sensitive potential responses toward the TMB oxidation catalyzed by peroxidase or its mimetics. The proposed electrode has been applied to peroxidase-labeled immunoassays and DNA hybridization assays based on the G-quadruplex/hemin DNAzyme beacon.

■ EXPERIMENTAL SECTION

Reagents and Materials. TMB, high-molecular-weight poly(vinyl chloride) (PVC), *o*-nitrophenyl octylether (*o*-NPOE), bis(2-ethylhexyl) sebacate (DOS), di-*n*-octyl phthalate (DOP), dinonylnaphthalene sulfonic acid (DNNS^-H^+) as a 50% solution in heptane, sodium tetraphenylborate (TPB^-) and other substituted tetraphenylborate salts, peroxidase from horseradish (Type VI, essentially salt-free, lyophilized powder, 256 U/mg solid), 2-[4-(2-hydroxyethyl)piperazin-1-yl]-

ethanesulfonic acid (HEPES) were purchased from Sigma–Aldrich. SiMAG-Goat antimouse IgG (1 μm in hydrodynamic diameter) was purchased from Chemicell. Mouse IgG and horseradish peroxidase (HRP)-labeled goat antimouse IgG were purchased from Beijing Solarbio Science and Technology Co., Ltd. Five DNA sequences were synthesized by Shanghai Sunny Biotech Co., Ltd. Other reagents were purchased from Sinopharm Group Co., Ltd. All chemicals were of selectophore grade or analytical reagent grade. Aqueous solutions were prepared with freshly deionized water (18.2 M Ω cm specific resistance) obtained with a Pall Cascada laboratory water system.

Electrode Preparation and EMF Measurements.

Polymeric liquid membranes containing *o*-NPOE and PVC in a weight ratio of 1:1 and a cation exchanger (0.015 mol/kg) were prepared by using a solvent-casting technique with tetrahydrofuran as the casting solvent. After transfer of the membrane cocktail to a glass ring fixed on a glass plate and evaporation of the tetrahydrofuran overnight, a uniform polymeric liquid membrane was obtained. Disks of 5 mm in diameter were punched from the parent polymeric liquid membrane and glued to plasticized PVC tubes (o.d. 5 mm, i.d. 3 mm) to fabricate the membrane electrodes. For measurements with phosphate buffer solutions (PBSs), 15 mM NaCl was used as the conditioning and inner filling solutions of the electrode. For measurements with HEPES– NH_4OAc –KCl–NaCl buffer (25 mM HEPES, 20 mM NH_4OAc , 10 mM KCl, 150 mM NaCl, pH 7.4), the same buffer was used as the conditioning and inner filling solutions.

All electromotive force (EMF) values were measured using a Model CHI 760C electrochemical workstation (Shanghai Chenhua Apparatus Corporation, China) in a Faraday cage in the following galvanic cell: Ag, AgCl/3 M KCl/1 M LiOAc/sample solution (well-stirred)/sensing membrane/inner filling solution/AgCl, Ag.

Liquid–Liquid Extraction Experiment. At 1 min after initiation of TMB oxidation (0.1 mM TMB, 0.5 mM H_2O_2 , 10^{-3} U/mL HRP) in 50 mM PBS of pH 7.4, 1 mL of this aqueous solution was mixed with 100 μL of *o*-NPOE doped with 1 mM DNNS^-H^+ . After vigorous shaking of the biphasic system for 15 s and spontaneous phase separation, a dense green organic phase (the liquid drop in Figure 1) and a clear aqueous phase were formed. The corresponding visible absorption spectra were measured with a Beckman Model DU-800 UV spectrophotometer and X-band EPR spectra were measured with a Bruker ESP300 Electron Spin Resonance spectrometer (the scan range was 3465 G to 3505 G).

Procedures of the Peroxidase-Labeled Sandwich Immunoassay. Magnetic microparticles coated with goat antimouse IgG (SiMAG-Goat antimouse IgG) were washed with phosphate-buffered saline (50 mM, pH 7.4) before use. Mouse IgG samples at different concentrations were incubated with the goat antimouse IgG-conjugated magnetic particles (the concentration of magnetic microparticles was 25 $\mu\text{g/mL}$) in phosphate-buffered saline containing 3% (w/w) BSA (total volume, 0.5 mL) for 1 h at 37 °C in the shaker. After washing three times with the phosphate-buffered saline with 0.05% (v/v) Tween-20, the magnetic microparticles were resuspended and incubated with an excess concentration of HRP-labeled goat antimouse IgG (5 $\mu\text{g/mL}$) for 1 h at the 37 °C shaker. After washing twice with the phosphate buffered saline with 0.05% (v/v) Tween-20 and once with the phosphate buffer solution (PBS, 50 mM, pH 5.5), the magnetic microparticles

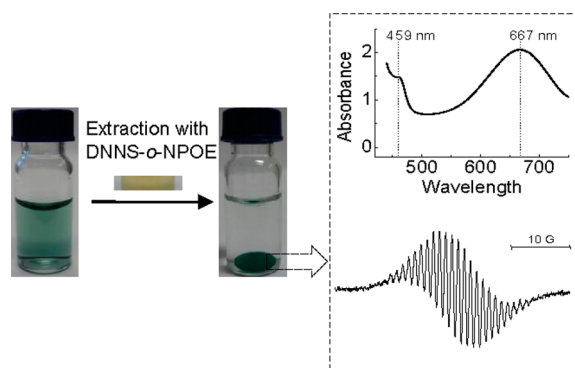


Figure 1. Liquid–liquid extraction experiment for TMB oxidation intermediates in a water-*o*-NPOE biphasic system mimicking the water–polymeric liquid membrane situation. The aqueous phase (left vial) is PBS of pH 7.4 containing HRP-catalyzed oxidation intermediates of TMB (0.1 mM TMB, 0.5 mM H₂O₂, 10^{−3} U/mL HRP, 1 min reaction). A *o*-NPOE solution of DNNS[−] was used to extract TMB oxidation intermediates from the aqueous phase. After efficient extraction and phase separation, the *o*-NPOE phase (the green liquid drop, right vial) was put into the microcuvette and capillary tube to take the visible absorbance (top spectrum) and EPR (bottom spectrum) measurements, respectively.

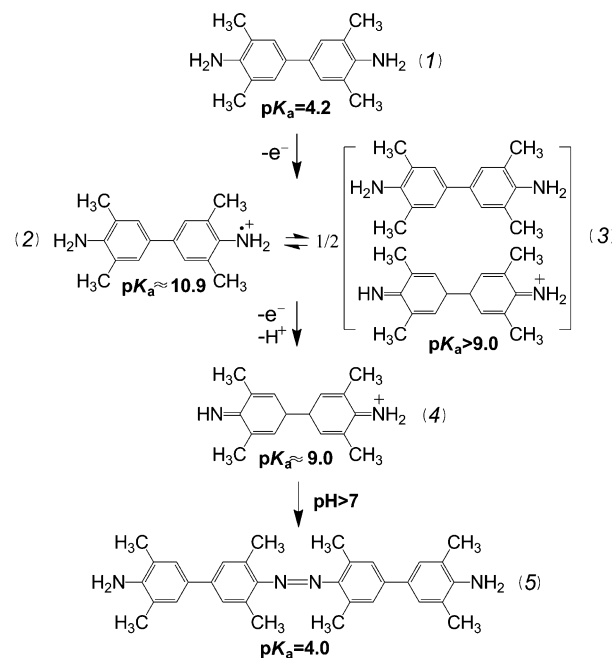
were resuspended in 0.5 mL PBS of pH 5.5 and transferred to a beaker. Then, 0.2 mM TMB and 1 mM H₂O₂ were added and the potential responses were recorded for 300 s. For control measurements, mouse IgG was replaced by BSA, and the potential response showed no significant difference from that in the blank experiment.

Procedures of the G-quadruplex DNAzyme-Based DNA Hybridization Assay. Two DNA probes (DNA1: 5′-ACAGGCGGCCTTAAGTGTAGTTGGGTAGGGCGGG-3′ and DNA2: 5′-TGGGTCTGGTGAATTGCTGCC-3′) both at a concentration of 75 nM and the target DNA (DNA3, 5′-GGCAGCAATTTACACAGTACTACAGTTAAGG-CCGCCTGT-3′) or the noncomplementary DNA at different concentrations (DNA4, 5′-CCGTCGTTAAAGTGGTCATG-ATGTCAATTCGGCGGACA-3′) in HEPES-NH₄OAc–KCl–NaCl buffer containing 1% dimethyl sulfoxide were heated at 95 °C for 5 min, and gradually cooled to room temperature. After a 1 h incubation with 50 nM hemin, 0.2 mM TMB and 10 mM H₂O₂ were added into the incubation solution and the potential responses on the TPB[−]-doped electrode were recorded for 60 s.

RESULTS AND DISCUSSION

In the presence of H₂O₂ and peroxidase or its mimetics, TMB (1) can be oxidized into its free radical form (2) via single electron transfer and converted to a diimine product (4) with further oxidation (Scheme 1). A charge transfer complex (3) of the diimine product (the electron acceptor) and the TMB substrate (the electron donor) is also formed in rapid equilibrium with the TMB radical.¹⁴ In HRP-labeled immunoassays and nucleic acid hybridization assays, as well as many inorganic peroxidase nanomimetic-based sensing strategies using TMB oxidation, signal readout steps are usually conducted at mildly acidic pHs (e.g., 4.0 to 5.5) to gain the optimal catalytic activity of peroxidase or peroxidase mimetics.² Under these conditions, the oxidized species of TMB can be quite stable. However, in recent years, homogeneous biosensing schemes based on peroxidase-mimicking DNAzymes have been rapidly developed, for which physiological pH conditions are

Scheme 1. Reaction Pathway of the H₂O₂-Mediated Oxidation of TMB Catalyzed by Peroxidase or Peroxidase Mimetics^a



^aFrom ref 16. See ref 17 for pK_a values.

favorable for signal readout steps due to the elimination of dilution steps. Also, the optimal pH values of G-quadruplex/hemin DNAzymes and some hemin-based peroxidase nanomimetics are higher than that of HRP, because of the high optimal pH for hemin, which are near neutral pHs.¹⁵ Under such conditions, the monomeric oxidized species of TMB can undergo further dimerization reaction and form a stable azo product (5),¹⁶ which is confirmed by the pseudo-molecular ion peak at *m/z* 477 in the ESI-mass spectrum (data not shown).

Scheme 1 also shows the pK_a of TMB and the intermediates and products generated in TMB oxidation. The pK_a values of the free radical (2), diimine (4), and charge transfer complex (3) are all several orders of magnitude higher than that of TMB (1). Under the commonly used mildly acidic and near-neutral pH conditions, TMB itself is mainly nonionic and cannot induce a large potential response on a polymeric liquid membrane electrode. However, these three monomeric oxidation intermediates are dominantly positively charged and possibly induce cationic potential responses on the membrane electrode. For the final azo dimer product (5) generated at a near-neutral pH, it is mainly nonionic according to its pK_a and thus cannot significantly contribute to the potential response as well. Moreover, log *P* values of the radical cation and the diimine cation were calculated to be 0.99 and 0.38, respectively, and the charge transfer complex should have a log *P* between that of TMB (4.02) and the diimine cation (0.38).¹⁸ These log *P* values indicate high lipophilicities of these TMB oxidation intermediates (e.g., higher than that of tetrapropylammonium ion with a log *P* of −0.45), which favor the potentiometric detection of them by hydrophobic polymeric liquid membranes.

Unlike a traditional polymeric liquid membrane electrode for a single stable ion (e.g., K⁺-selective electrode), the cationic species in the TMB oxidation may contribute to the potential responses together. Therefore, to obtain their potential

responses, the cation exchanger-doped electrode cannot be conditioned by a single primary ion (i.e., target ion) as for the classical ion-selective electrode. Rather, the polymeric liquid membrane can be conditioned by the background ion. This conditioning mode has been used in our recently developed electrodes responsive to intermediates generated in oxidations of *N,N',N,N'*-tetramethylbenzidine and *o*-phenylenediamine.^{13d,15c} For these background ion-conditioned membrane electrodes, the heterogeneous ion exchange of cationic intermediates in the sample phase with the background cation (e.g., Na^+) in the membrane is the prerequisite for potential responses. However, because of the high reactivity of the previously investigated oxidation intermediates, no evidence has been provided for the ion exchange processes. Here, the three cationic species in H_2O_2 -mediated TMB oxidation are less transient and amenable to characterization. Therefore, their heterogeneous ion exchange processes were first examined.

The visible absorbance and EPR spectra were first measured for the PBS (pH 7.4) with the enzymatically generated TMB oxidation intermediates before the liquid–liquid extraction experiment. The characteristic signals of three oxidation intermediates have been obtained (see Figure S1 in the Supporting Information), which agree with the previously reported spectra.^{14,16} When such an aqueous phase was effectively mixed with *o*-NPOE containing DNNS[−], the characteristic absorption spectra of the diimine (with an absorption peak at 459 nm) and the charge-transfer complex (with an absorption peak at 667 nm) were clearly observed in *o*-NPOE after phase separation. Via EPR spectroscopy, a strong characteristic signal of the TMB radical was obtained in the *o*-NPOE phase.¹⁴ These evidences indicate that the cationic species generated in the TMB oxidation are indeed capable of being transferred to the cation exchanger-doped organic phase. Moreover, when extracted by pure *o*-NPOE without ion exchanger, these cations mainly existed in the aqueous phase after extraction (data not shown).¹⁹ The heterogeneous ion exchange process may be facilitated by the cation exchanger in the organic phase via formation of cooperative ion pairs with the positively charged oxidation intermediates.

According to the phase boundary potential theory,²⁰ the heterogeneous ion exchanges of cationic species across the sample/membrane interface would induce potential responses on the polymeric liquid membrane electrode. As shown in Figure 2A (solid line), a large cationic potential response was observed upon the oxidation of TMB by HRP/ H_2O_2 system in PBS (pH 5.5) on the DNNS[−]-doped electrode. After 1 h of reaction, a large potential response (dashed line) could still be obtained, because of the relatively good stability of the cationic oxidized species of TMB. However, when the TMB oxidation reaction was conducted at the physiological pH, the oxidized species become less stable and their potential response became an “intermediate” response similarly with those of oxidation intermediates of *N,N,N',N'*-tetramethylbenzidine and *o*-phenylenediamine.^{13d,15c} As shown in Figure 2B, although the real-time potential response (solid line) of TMB oxidation is large in PBS of pH 7.4, the potential response toward the 1 h reaction mixture (dashed line) becomes much smaller because the monomeric oxidation intermediates significantly convert to the nonionic azo dimer product. Also, the potential responses of TMB oxidation mixtures in PBS of pH 7.4 at different reaction time points within 2 h show the successive attenuation of potential signals over time (see Figure S2 in the Supporting Information), which further confirms the instability of species

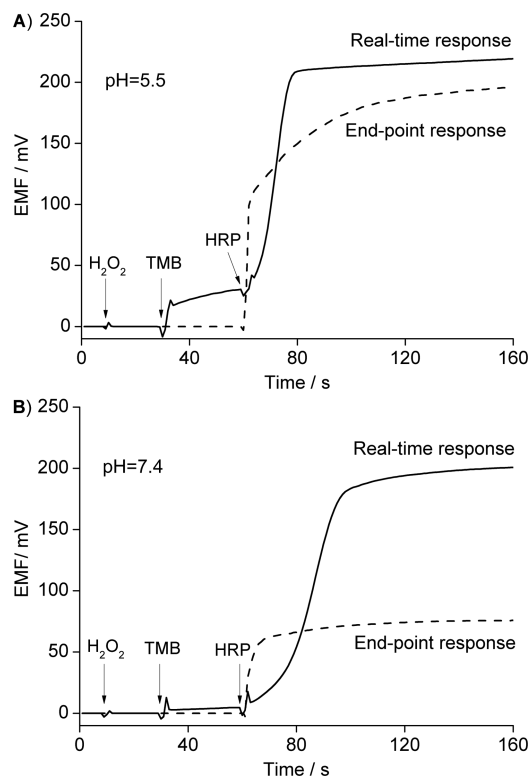


Figure 2. Real-time potential responses toward the HRP-catalyzed TMB oxidation (0.1 mM TMB, 0.5 mM H_2O_2 , 10^{-3} U/mL HRP) and end-point potential responses to the reaction products on the DNNS[−]-doped electrode in 50 mM PBS of (A) pH 5.5 and (B) pH 7.4. The end-point potential responses were obtained by placing the electrode in the 1-h-reaction mixture under the same conditions as those used for real-time responses.

responsible for the potential responses under near-neutral pH conditions.

Notably, DNNS[−] was used as the ion exchanger to demonstrate the phase transfer of cations and the basic principle of potential responses because cationic intermediates of TMB oxidation show better stability in DNNS[−]-doped *o*-NPOE than *o*-NPOE doped with TPB[−] or substituted TPB[−]. The better stability benefits the characterization of these intermediates (especially EPR measurements). The different stabilities of the intermediates in the presence of different ion exchangers are probably due to the fact that better steric accessibility of sulfonate group allows for stronger ion-pair interactions with positively charged species²¹ and the ion-pair interactions can stabilize the cationic intermediates in aromatic amine oxidations.²² However, potential responses of these cationic intermediates in a certain background electrolyte are also related to more factors such as other intermolecular interactions of the ion exchanger with the intermediates (e.g., π – π interaction) and the binding affinity of the ion exchanger with the background cation (i.e., Na^+). Here, TPB[−] as the ion exchanger of the polymeric liquid membrane electrode shows better response sensitivity toward the TMB oxidation, compared to DNNS[−] (see Figure S3 in the Supporting Information), which is similar to the electrode sensitive to chemically stable alkyl-ammonium cations²³ and *o*-phenylenediamine oxidation.^{15c} Therefore, the TPB[−]-based membrane electrode is used in further biosensing applications. In addition, *o*-NPOE as the plasticizer of the membrane has been found to show better response sensitivity, compared to less-

polar plasticizers (see Figure S4 in the Supporting Information).

Because of the difficulty in obtaining a pure and stable intermediate, the direct characterization (e.g., selectivity and lower detection limit) of the electrode responsive to the TMB oxidation intermediates is difficult, using established methods for classical ion-selective electrodes. However, the oxidation of TMB at a concentration of 10^{-6} M was found to induce a cationic potential response of more than 30 mV in 50 mM PBS of pH 7.4 (see Figure S5 in the Supporting Information). Because the total concentration of TMB oxidation intermediates is lower than the initial TMB concentration, the detection limit of the electrode toward TMB oxidation intermediates should be lower than 10^{-6} M.

To regenerate the discriminated ion-conditioned electrode after measurements, high concentrations of salts and ethanol (e.g., a mixture of 2 M aqueous NaCl solution and ethanol (4:1, v:v)) could be used to extract neutral TMB and cationic oxidation products out of the membrane. However, a long washing time (e.g., 30 min) is required and TPB[−] may suffer from limited long-term stability. Therefore, the ion exchanger-doped electrodes were always singly used here. Since the electrodes without ionophores are quite cost-effective and easy to prepare, the single use is acceptable in practical applications.

Based on the potential responses induced by H₂O₂-mediated TMB oxidations, the proposed electrode can be used to determine the catalytic activities of peroxidase and peroxidase mimetics and further develop related biosensing schemes. HRP is one of the most commonly used amplifying labels in immunoassays. However, HRP-labeled immunoassays based on polymeric liquid membrane electrodes are rather rare, probably due to the lack of peroxidase-catalyzed reactions showing sensitive potential responses on this type of electrode. Herein, the polymeric liquid membrane electrode responsive to TMB oxidation was examined as the potentiometric indicator electrode for a model sandwich HRP-labeled immunoassay (Figure 3A). The target antigen (mouse IgG) was first captured by the magnetic microbeads modified with the capture antibody (goat antimouse IgG). Then, the detection antibody (goat antimouse IgG labeled with HRP) was added to bind with the antigen. After washing the excessive HRP-labeled detection antibody, the catalytic activity of HRP immobilized on the magnetic microbeads for H₂O₂-mediated TMB oxidation was measured by the polymeric liquid membrane electrode. As shown in Figure 3B, as the concentration of target antigen increases, the cationic potential response increases. The potential increase measured at 5 min after initiation of TMB oxidation was used for quantification. The calibration curve for mouse IgG was plotted as the inset of Figure 3B. The linear range for detection of mouse IgG is 0.3–30 ng/mL and the detection limit is 0.02 ng/mL (3σ). This detection limit is 2 orders of magnitude lower than those obtained by the potentiometric immunoassays using nanoparticle labels and low-detection-limit ion-selective electrodes.²⁴

Considering the wide utility of G-quadruplex/hemin DNAzymes in bioanalysis, the feasibility of the TMB oxidation-sensitive electrode in sensing G-quadruplex/hemin DNAzymes and DNAzyme-involved biorecognition events has been examined. As shown in Figure 4, in the presence of the model G-quadruplex/hemin DNAzyme,²⁵ a large potential response can be obtained toward the H₂O₂-mediated TMB oxidation, while hemin (with limited peroxidase-like activity) or G-rich sequence (with no catalytic activity) as the catalyst could

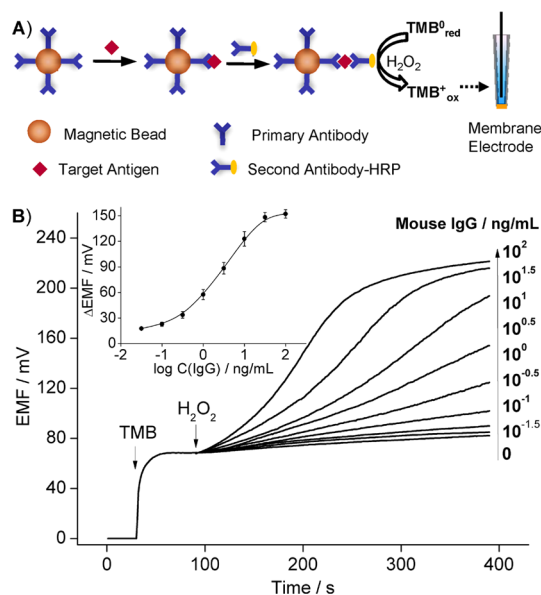


Figure 3. (A) Schematic representation of the potentiometric sandwich immunoassay on magnetic microbeads; (B) potential responses of the TMB oxidation (0.2 mM TMB, 1 mM H₂O₂) on the TPB[−]-doped electrode for increasing concentrations of mouse IgG in PBS (pH 5.5). The inset shows the calibration curve for potentiometric mouse IgG detection. Each error bar represents one standard deviation for three measurements.

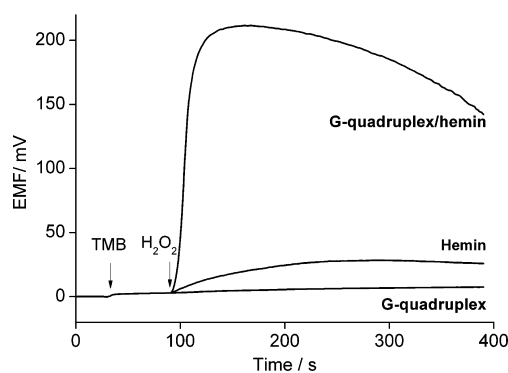


Figure 4. Potential responses of the H₂O₂-mediated oxidation of TMB catalyzed by the G-quadruplex/hemin complex, hemin, and G-quadruplex. Experimental conditions: HEPES-NH₄OAc-KCl-NaCl buffer, pH 7.4; G-rich DNA (5′-GGGTAGGGCGGGTTGGGT-3′), 50 nM; hemin, 50 nM; TMB, 0.2 mM; H₂O₂, 10 mM. Before measurements, the catalysts were incubated in the buffer for 0.5 h.

only induce small or negligible potential responses. Based on the superior peroxidatic activity of the G-quadruplex/hemin DNAzyme, a label-free potentiometric DNA hybridization assay protocol has been developed. Two DNA probes both with a recognition sequence that can hybridize with a part of the target DNA and another read-out sequence that can be combined to a G-quadruplex were used (see Figure 5A).²⁶ The hybridization of target DNA with two DNA probes can promote two overhanging split G-rich sequences to assemble to the G-quadruplex. In the presence of hemin, the G-quadruplex shows peroxidase-like activity and catalyzes the H₂O₂-mediated oxidation of TMB, which further induces potential responses on the cation exchanger-doped electrode. As shown in Figure 5B, with increasing concentrations of target DNA, increasing cationic potential responses can be obtained, which results from

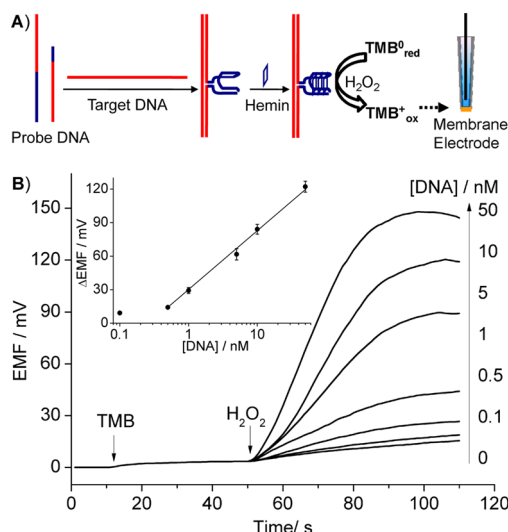


Figure 5. (A) Schematic representation of the DNA hybridization assay using two DNA probes with split G-quadruplex-forming sequences; (B) potential responses of the TMB oxidation (0.2 mM TMB, 10 mM H₂O₂) on the TPB[−]-doped electrode for increasing concentrations of target DNA in HEPES-NH₄OAc-KCl-NaCl buffer (pH 7.4). The inset shows the calibration curve for potentiometric DNA detection. Each error bar represents one standard deviation for three measurements.

the increasing amounts of assembled G-quadruplex/hemin DNAzyme. For a noncomplementary DNA sequence at a concentration up to 10^{−7} M, negligible potential responses were obtained, compared to that of the blank sample (data not shown). Using the potential increase measured at 30 s after initiation of TMB oxidation for quantification, the calibration curve for detection of the target DNA was plotted as the inset in Figure 5. As can be seen, the target DNA can be detected with a linear range of 0.5–50 nM and a detection limit of 0.1 nM (3σ). This detection limit is at least 1 order of magnitude lower than those obtained by spectrophotometric and fluorometric DNA hybridization assays using the similar G-quadruplex/hemin DNAzyme-based principles.^{26,27}

CONCLUSIONS

A potentiometric transduction technique for TMB oxidation has been developed using potential responses of cationic species in TMB oxidation on the polymeric liquid membrane electrode functionalized by an appropriate lipophilic cationic exchanger. This method has been successfully used in peroxidase and peroxidase-mimicking DNAzyme-based biosensing systems including immunoassays and DNA hybridization assays with high detection sensitivities. Since the potential responses of the proposed electrode are based on accumulation of cationic species in the interfacial layer of the membrane, approaches that can enhance the mass transfer from the sample solution to the sample-membrane interface (e.g., rotating electrode configuration) or suppress the ion diffusion from the interface into the membrane bulk (e.g., use of more rigid membrane) are expected to further improve the sensitivities of this method.²⁸ With the demonstrated phase transfer behaviors of cationic species in TMB oxidation, other electrochemical techniques for liquid–liquid biphasic systems (e.g., voltammetry and chronoamperometry at liquid/liquid interfaces)^{11,29} can also be utilized to indicate the TMB

oxidation for the development of related analytical and bioanalytical protocols.

ASSOCIATED CONTENT

Supporting Information

Additional information as noted in text. This material is available free of charge via the Internet at <http://pubs.acs.org>.

AUTHOR INFORMATION

Corresponding Author

*E-mail: wqin@yic.ac.cn.

Notes

The authors declare no competing financial interest.

ACKNOWLEDGMENTS

We thank Dr. Yanhong Liu (The Technical Institute of Physics and Chemistry of the Chinese Academy of Sciences) for her technical support for EPR measurements. This work was financially supported by the Instrument Developing Project of the Chinese Academy of Sciences (No. YZ201161), the National Natural Science Foundation of China (No. 41176081), and the Taishan Scholar Program of Shandong Province (No. TS20081159).

REFERENCES

- (1) (a) Mesulam, M. M. *J. Histochem. Cytochem.* **1978**, *26*, 2106–2117. (b) Bos, E. S.; Van der Doelen, A. A.; Rooy, N. V.; Schuur, A. H. W. M. *J. Immunoassay Immunochem.* **1981**, *2*, 187–204. (c) Porstmann, T.; Kiessig, S. T. *J. Immunol. Methods* **1992**, *150*, 5–21.
- (2) (a) Gao, L.; Zhuang, J.; Nie, L.; Zhang, J.; Zhang, Y.; Gu, N.; Wang, T.; Feng, J.; Yang, D.; Perrett, S.; Yan, X. *Nat. Nanotechnol.* **2007**, *2*, 577–583. (b) Liu, G.; Wan, Y.; Gau, V.; Zhang, J.; Wang, L.; Song, S.; Fan, C. *J. Am. Chem. Soc.* **2008**, *130*, 6820–6825. (c) Ngo, T. T. *Anal. Lett.* **2010**, *43*, 1572–1587.
- (3) (a) Willner, I.; Shlyahovsky, B.; Zayats, M.; Willner, B. *Chem. Soc. Rev.* **2008**, *37*, 1153–1165. (b) Park, K. S.; Kim, M. I.; Cho, D. Y.; Park, H. G. *Small* **2011**, *7*, 1521–1525. (c) Lv, L.; Guo, Z. J.; Wang, J. H.; Wang, E. K. *Curr. Pharm. Des.* **2012**, *18*, 2076–2095. (d) Xie, J.; Zhang, X.; Wang, H.; Zheng, H.; Huang, Y. *TrAC Trends Anal. Chem.* **2012**, *39*, 114–129.
- (4) (a) Arapova, G. S.; Eryomin, A. N.; Metelitz, D. I. *Biochemistry (Moscow)* **1997**, *62*, 1415–1423. (b) Tsuji, A.; Teshima, N.; Kurihara, M.; Nakano, S.; Kawashima, T. *Talanta* **2000**, *52*, 161–167. (c) Slocumbe, L. L.; Colditz, I. G. *Food Agr. Immunol.* **2011**, *22*, 135–143. (d) Zhao, J.; Xie, Y.; Yuan, W.; Li, D.; Liu, S.; Zheng, B.; Hou, W. J. *Mater. Chem. B* **2013**, *1*, 1263–1269. (e) Zhang, J.; Yang, C.; Chen, C.; Yang, X. *Analyst* **2013**, *138*, 2398–2404.
- (5) (a) Song, Y.; Qu, K.; Zhao, C.; Ren, J.; Qu, X. *Adv. Mater.* **2010**, *22*, 2206–2210. (b) Ding, N.; Yan, N.; Ren, C.; Chen, X. *Anal. Chem.* **2010**, *82*, 5897–5899. (c) Wang, X.; Wu, Q.; Shan, Z.; Huang, Q. *Biosens. Bioelectron.* **2011**, *26*, 3614–3619. (d) Liang, M.; Fan, K.; Pan, Y.; Jiang, H.; Wang, F.; Yang, D.; Lu, D.; Feng, J.; Zhao, J.; Yang, L.; Yan, X. *Anal. Chem.* **2013**, *85*, 308–312.
- (6) (a) Mesquita, R. B.; Noronha, M. L. F. O. B.; Pereira, A. I.; Santos, A. C.; Torres, A. F.; Cerdà, V.; Rangel, A. O. *Talanta* **2007**, *72*, 1186–1191. (b) Zhang, J.; Yang, X. *Analyst* **2013**, *138*, 434–427.
- (7) (a) Semin, B. K.; Seibert, M. *Photosynth. Res.* **2009**, *100*, 45–48. (b) Jang, G. G.; Roper, D. K. *Anal. Chem.* **2011**, *83*, 1836–1842. (c) Liu, X.; Wang, Q.; Zhang, Y.; Zhang, L.; Su, Y.; Lv, Y. *New J. Chem.* **2013**, *37*, 2174–2178. (d) Hou, X. L.; Li, J. L.; Drew, S. C.; Tang, B.; Sun, L.; Wang, X. G. *J. Phys. Chem. C* **2013**, *117*, 6788–6793.
- (8) (a) Laing, S.; Hernandez-Santana, A.; Sassmannshausen, J.; Asquith, D. L.; McInnes, I. B.; Faulds, K.; Graham, D. *Anal. Chem.* **2011**, *83*, 297–302. (b) McKeating, K. S.; Graham, D.; Faulds, K. *Chem. Commun.* **2013**, *49*, 3206–3208.

- (9) (a) Volpe, G.; Compagnone, D.; Draisci, R.; Palleschi, G. *Analyst* **1998**, 123, 1303–1307. (b) Fanjul-Balado, P.; González-García, M. B.; Costa-García, A. *Anal. Bioanal. Chem.* **2005**, 382, 297–302. (c) Baldrich, E.; del Campo, F. J.; Munoz, F. X. *Biosens. Bioelectron.* **2009**, 25, 920–926. (d) Sun, W.; Ju, X.; Zhang, Y.; Sun, X.; Li, G.; Sun, Z. *Electrochem. Commun.* **2013**, 26, 113–116.
- (10) Martin, S. P.; Lynch, J. M.; Reddy, S. M. *Biosens. Bioelectron.* **2002**, 17, 735–739.
- (11) (a) Smith, P. J. S. *Nature* **1995**, 378, 645–646. (b) Bakker, E.; Pretsch, E. *Angew. Chem., Int. Ed.* **2007**, 46, 5660–5668. (c) Bakker, E.; Pretsch, E. In *Electroanalytical Chemistry, A Series of Advances*; Bard, A. J., Zoski, C. G., Eds.; CRC Press: Boca Raton, FL, 2012; pp 1–74.
- (12) (a) Dorazio, P.; Rechnitz, G. A. *Anal. Chem.* **1977**, 49, 2083–2086. (b) Meyerhoff, M.; Rechnitz, G. A. *Science* **1977**, 195, 494–495. (c) Shiba, K.; Watanabe, T.; Umezawa, Y.; Fujiwara, S.; Momoi, H. *Chem. Lett.* **1980**, 9, 155–158.
- (13) (a) Eggins, B. R. *Chemical Sensors and Biosensors; Analytical Techniques in the Sciences*; Wiley: Chichester, England, 2002; pp 125–138. (b) Numnuam, A.; Chumbimuni-Torres, K. Y.; Xiang, Y.; Bash, R.; Thavarungkul, P.; Kanatharana, P.; Pretsch, E.; Wang, J.; Bakker, E. *J. Am. Chem. Soc.* **2008**, 130, 410–411. (c) Szűcs, J.; Pretsch, E.; Gyurcsányi, R. E. *Analyst* **2009**, 134, 1601–1607. (d) Wang, X. W.; Qin, W. *Chem. Commun.* **2012**, 48, 4073–4075. (e) Wang, X. W.; Wang, Q.; Qin, W. *Biosens. Bioelectron.* **2012**, 38, 145–150. (f) Wang, X. W.; Ding, Z. F.; Ren, Q. W.; Qin, W. *Anal. Chem.* **2013**, 85, 1945–1950.
- (14) Josephy, P. D.; Eling, T.; Mason, R. P. *J. Biol. Chem.* **1982**, 257, 3669–3675.
- (15) (a) Li, B.; Du, Y.; Li, T.; Dong, S. *Anal. Chim. Acta* **2009**, 651, 234–240. (b) Song, Y.; Chen, Y.; Feng, L.; Ren, J.; Qu, X. *Chem. Commun.* **2011**, 47, 4436–4438. (c) Wang, X.; Qin, W. *Chem.—Eur. J.* **2013**, 19, 9979–9986.
- (16) (a) Josephy, P. D.; Mason, R. P.; Eling, T. *Cancer Res.* **1982**, 42, 2567–2570. (b) Gao, L.; Wu, J.; Gao, D. *ACS Nano* **2011**, 5, 6736–6742.
- (17) (a) pK_a of TMB: Chung, K. T.; Chen, S. C.; Wong, T. Y.; Li, Y. S.; Wei, C. I.; Chou, M. W. *Toxicol. Sci.* **2000**, 56, 351–356. (b) pK_a of the free radical: Dey, G. R.; Naik, D. B.; Kishore, K.; Moorthy, P. N. *Radiat. Phys. Chem.* **1994**, 43, 481–485. (c) pK_a of the diimine: McClelland, R. A.; Ren, D.; D'Sa, R. A.; Ahmed, A. R. *Can. J. Chem.* **2000**, 78, 1178–1185. (d) Because of the electron-donating effect of parent diamine on quinone diimine in charge-transfer complex, pK_a of charge-transfer complex is larger than that of the electron acceptor: Nishina, Y.; Sato, K.; Tamaoki, H.; Tanaka, T.; Setoyama, C.; Miura, R.; Shiga, K. *J. Biochem.* **2003**, 134, 835–842. (d) pK_a of the azo dimer: ACD/PhysChem Suite, Version 6.0; Advanced Chemistry Development, Inc.: Toronto, ON, Canada, 2002.
- (18) Calculator Plugins for structure property prediction, Marvin, ChemAxon, Budapest, Hungary, 2014; <http://www.chemaxon.com/demosite/marvin/index.html> (accessed March 3, 2014).
- (19) No characteristic signals for three cationic species could be obtained in the organic phase after extraction. However, the undetectable characteristic signals of oxidation products do not simply mean no extraction and may be due to the instability of these species in pure organic phase. According to the concentration of these species left in the aqueous phase after extraction, less than 50% of them were extracted into the organic phase, compared to the high extraction efficiency (larger than 90%) using DNNS-doped NPOE.
- (20) Bakker, E.; Bühlmann, P.; Pretsch, E. *Talanta* **2004**, 63, 3–20.
- (21) Egorov, V. V.; Lyaskovski, P. L.; Il'inchik, I. V.; Soroka, V. V.; Nazarov, V. A. *Electroanalysis* **2009**, 21, 2061–2070.
- (22) Kireiko, A. V.; Veselova, I. A.; Shekhovtsova, T. N. *Russ. J. Bioorg. Chem.* **2006**, 32, 71–77.
- (23) Egorov, V.; Bolotin, A. *J. Anal. Chem.* **2006**, 61, 279–283.
- (24) (a) Chumbimuni-Torres, K. Y.; Dai, Z.; Rubinoya, N.; Xiang, Y.; Pretsch, E.; Wang, J.; Bakker, E. *J. Am. Chem. Soc.* **2006**, 128, 13676–13677. (b) Thürer, R.; Vigassy, T.; Hirayama, M.; Wang, J.; Bakker, E.; Pretsch, E. *Anal. Chem.* **2007**, 79, 5107–5110.
- (25) Nakayama, S.; Wang, J.; Sintim, H. O. *Chem.—Eur. J.* **2011**, 17, 5691–5698.
- (26) Deng, M. G.; Zhang, D.; Zhou, Y. Y.; Zhou, X. *J. Am. Chem. Soc.* **2008**, 130, 13095–13102.
- (27) (a) Xiao, Y.; Pavlov, V.; Niazov, T.; Dishon, A.; Kotler, M.; Willner, I. *J. Am. Chem. Soc.* **2004**, 126, 7430–7431. (b) Qiu, B.; Zheng, Z. Z.; Lu, Y. J.; Lin, Z. Y.; Wong, K. Y.; Chen, G. N. *Chem. Commun.* **2011**, 47, 1437–1439.
- (28) (a) Ramamurthy, N.; Baliga, N.; Wahr, J. A.; Schaller, U.; Yang, V. C.; Meyerhoff, M. E. *Clin. Chem.* **1998**, 44, 606–613. (b) Ye, Q. S.; Meyerhoff, M. E. *Anal. Chem.* **2001**, 73, 332–336. (c) Qin, W.; Liang, R. N.; Fu, X. L.; Wang, Q. W.; Yin, T. J.; Song, W. J. *Anal. Chem.* **2012**, 84, 10509–10513.
- (29) Liu, S.; Li, Q.; Shao, Y. *Chem. Soc. Rev.* **2011**, 40, 2236–2253.